THREE-STEP REGISTRATION AND MULTI-THREAD PROCESSING BASED IMAGE MOSAIC FOR UNMANNED AERIAL VEHICLE APPLICATIONS

Hongguang Li [1,2], Wenrui Ding [1, 3], and Yufeng Wang [4]
[1] Research Institute of Unmanned Aerial Vehicle, Beihang University, Beijing 100191, China
[2] School of Mechanical Engineering and Automation, Beihang University, Beijing 100191, China
[3] Collaborative Innovation Center of Geospatial Technology, Wuhan 430000, China
[4] School of Electronic and Information Engineering, Beihang University Beijing 100191, China
E-Mail: dwr_buaa@163.com

Submitted: Nov. 30, 2015 ***Accepted: Apr. 2, 2016*** ***Published: June 1, 2016***

Abstract- In the area of image mosaic for unmanned aerial vehicle (UAV) applications, the problems of precision and time consumption have drawn many scholars' attention. To address above two problems, a novel algorithm based on three-step registration and multi-thread processing is proposed in this paper. This method divides the image registration into three steps to improve the precision. Firstly, based on the SIFT features, the fast index mechanism k-d tree and the Euclidean distance are utilized to determine the common points between two adjacent images; then, the linear slope constraint model is used to filter the mismatching point-pairs; finally, the RANSAC algorithm is adopted to remove outer points from the common points to ensure matching precision of inter frames. To accommodate the real time requirement of UAV application, a parallel data processing pattern is presented. The multi-core resources and multi-thread computing method of computers are employed adequately in the new pattern to speed up the whole algorithm. Extensive experiments on precision and time consumption show the superior performance of the proposed algorithm.

Index terms*:* UAV; image mosaic; image registration; multi-thread processing.

I. INTRODUCTION

1.1 Background

Unmanned Aerial Vehicles Remote Sensing (UAVRS) is a kind of remote sensing technology, which has its own advantages compared with the satellite surveillance technology, such as low cost, flexible control of surveillance area and unrestricted access time, and the available remote sensing images obtained by UAVs have the characteristics of rich information and high resolution [1]. Therefore, UAVs have been widely used in the field of environmental monitoring [2], natural disaster area assessment [3] and battlefield surveillance [4] in recent years.

And the UAVRS platform for ordinary digital camera has become one of the most important focuses in scientific research and application. But because of small field of view and high overlap rate of UAV vision, it is difficult to use a single frame to reflect entire information of the region of interest (ROI). In order to get more effective and comprehensive information from the UAV image data, image mosaic need to be carried out has become one of the key techniques in image reconstruction.

Given the different conditions of UAV photogrammetric flight and the geometric positioning, the aerial images may vary greatly for different times. So it is important to solve the mosaic precision problem of mosaic seam dislocations caused by error accumulation. Meanwhile, with the amount of data constantly increasing rapidly, it is difficult to address the problem of poor real-time capability caused by large amount of calculation. Consequently, the fast and efficient integration of images puts forward higher requirements for the processing of image mosaic.

1.2 Related Work

At present, the theoretical basis is mature in the field of image mosaic. The most popular are feature based method. In 2004, Lowe proposed the scale-invariant feature transform (SIFT) algorithm [5], which is currently the most widely used image registration algorithm. Although this algorithm has a good registration effect [6], it has not effectively improved the speed of image mosaic. Most scholars improve the speed index from parameter configurations of the SIFT algorithm [7-8], which cannot fully achieve real-time processing effect. The Speeded-Up Robust Features (SURF) algorithm proposed by H. Bay is several times faster than SIFT and has robust image transformation [9], but it is still time-consuming because of its float feature vector. The

ORB algorithm proposed by Rublee E is rotation and scale invariant with improved execution time, while sacrificing very little on performance accuracy [10].

As an important research direction of image reconstruction, image mosaic has been widely studied. The traditional mosaic system for UAV remote sensing image takes a lot of time and man power, it is difficult to complete the image stitching automatically. An approach for geometric correction of remote sensing image without any ground control points was presented in paper [11], and an automatic mosaic system for UAV remote sensing video images are deployed. A method combining SURF, FLANN trees and RANSAC algorithms to detect interest points, match those interest points and eliminate mismatch points for image registration was presented [12]. Paper [13] proposed automated image mosaicking method based on SFM was proposed in, calculating the camera parameters and 3D coordinates of feature points on basis of a set of pre-processing. In paper [14], a fusion algorithm of SAR and optical image with fast sparse representation on low-frequency images was proposed, and a sparse decomposition process is improved to reduce the algorithm running time. Paper [15] proposed an approach based on structure deformation and propagation for achieving the overall consistency in image structure and intensity. Paper [16] presented an algorithm employing Harris Corner Detection for detecting the key point and using the RANSAC method to choose the closest match between the two images by separating inliers and outliers.

Most scholars above tried to eliminate the mosaicking errors and reduce the amount of computation. With the real-time requirement of the geographic information for emergency events and safeguard, the real-time processing of UAV surveillance images is becoming increasingly prominent. Designing a method that can both improve the mosaicking speed and guarantee the mosaicking precision is the key problem in the process of image reconstruction.

1.3 Work in This Paper

Aiming at the problem of error accumulation and mosaic dislocation, and the problem of large amount of data and poor real-time property, this paper presents a novel algorithm based on three-step registration and multi-thread processing. On the basis of SIFT feature detection, the transformation matrix of high precision is obtained and the mosaic error accumulation is eliminated by the Euclidean distance, linear slope constraint and RANSAC algorithm [18]. Meanwhile, the multi-core resources of computer are utilized to create multi threads, design the

acceleration method of image mosaic and realize fast mosaic processing to meet real-time requirement of UAV applications. Extensive experiments on mosaic precision and time consumption are carried out and the results are quite encouraging.

II. METHODOLOGY

2.1 Parallel Processing Analysis

The processing flow of traditional image mosaic methods based on SIFT features mainly consists of three key parts, including feature extraction, feature matching and image fusion. Image feature extraction is a procedure that each image is disposed separately, and feature points extracted from each image are stored in the corresponding memory area. Image feature points are independent of each other, only as the feature matching input of adjacent images. In terms of the UAV images, the number of feature points extracted from a single image is quite large, even up to tens of thousands, creating large amount of calculation. Therefore, the fact that image feature extraction meets the conditions of parallel processing is determined by two aspects, namely, feature extraction being a special link of image mosaic process and having large amount of calculation. And relevant experimental results show that in the process of image mosaic, feature extraction is the most time-consuming step. The consuming time of each part is shown in Table 1.

Table 1. Proportion distribution of consuming time in mosaic

Process	Time-consuming percentage of total time
Feature extraction	50%
Feature matching	10%
Image fusion	40%

Consequently, in the process of image mosaic, we use multi-thread method to extract the feature points of images to reduce the time consumption of feature extraction.

2.2 Task Distribution of Multi Threads

In image mosaic, image feature extraction is the most time-consuming step, and there is no dependent relationship between the feature points of two adjacent images, which meets the

conditions of parallel processing. Therefore, the multi-core resources of processors could be utilized to complete the parallel processing of image feature extraction[17], as shown in Figure 1.

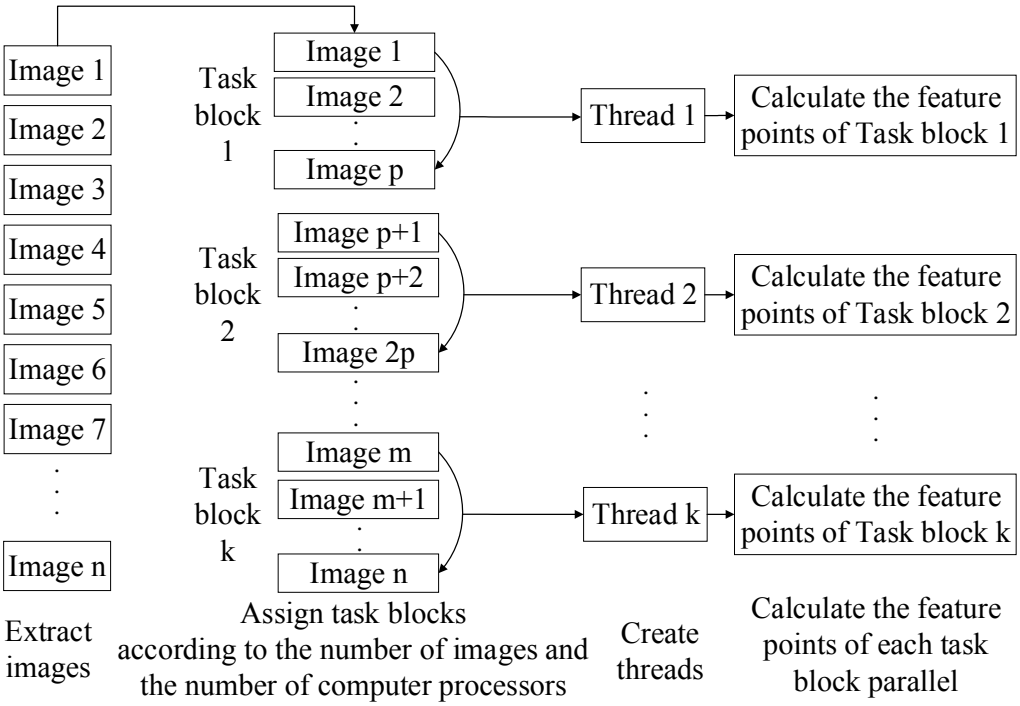

Figure 1. Task distribution in features extraction

First, the images were extracted from UAV videos. Then, according to the number of images and the number of processor cores, the images are divided into k task blocks equally, namely, the images to be processed are divided into k groups. Ideally, the number of images in each group should be equal, forming k task blocks. Finally, multi threads are created according to the number of assigned task blocks. The k blocks work parallel, and are used to extract the feature points, extracted by SIFT algorithm, of the images from the corresponding task block.

Assuming that the time to complete the task block of each thread is T_i, $i = 1,2,3,.....,k$, the time of using multi-thread parallel processing to calculate the feature points of n images should be $T_p = \max(T_1, T_2, ..., T_k)$, which is shortened a lot compared with the consuming time, $T_s = T_1 + T_2 + \ldots + T_k$, of serial processing. Meanwhile, the more computer processor cores are, the more threads can be created, and the shorter time of processing would be.

2.3 Three-step Registration

The image mosaic seams are mainly caused by the mismatching in image mosaic process and the error accumulation in registration. After ratio purification and RANSAC algorithm [13] registration, some mismatching points among the feature points extracted from mosaic images still exist, resulting in inaccuracy of the calculating transformation matrix. Meanwhile, the mosaic process is always based on the first frame image, and the subsequent images are transformed by the transition matrix into the coordinate system of the first frame image. If the transformation matrix is imprecise, it might lead to errors in image transformation process, and produce mosaic seams. Thus，determining accurate feature point-pairs is an important part of image registration and mosaic process. In order to achieve desired registration precision of the feature points between adjacent images, this paper proposes a three-step registration method to gradually eliminate the mismatching points between adjacent images, as shown in Figure 2.

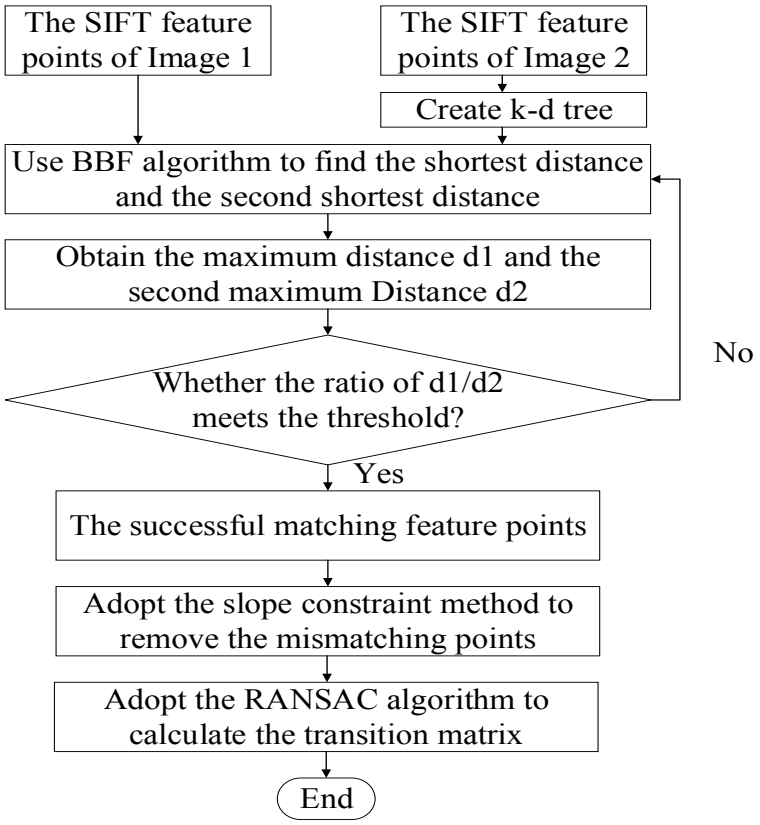

Figure 2. The flow chart of three-step registration method

Firstly, the fast indexing mechanism k-d tree is established based on the BBF priority search algorithm [19]. The ratio purification method which calculates the Euclidean distance between the feature vectors is utilized to preliminarily determine the common points between two adjacent images. All feature points extracted from the second image to be matched (denoted as $P_i^2, i = 1,2,3,...,N_2$, N_2 represents the number of feature points in the second image) is used to construct the k-d tree. Based on the k-d tree constructed in Figure 2, the BBF algorithm with the function of searching priority is used to search the feature points to be matched (denoted as $P_j^1, j = 1,2,3,...,N_1$, N_1 represents the number of feature points in the first image) in the first image. The feature points with the shortest and the second shortest Euclidean distance between the 128 dimension feature point descriptor corresponding to P_j^1 be searched, and the Euclidean distances between them are calculated as the shortest distance d_0 and the second shortest distance d_1 respectively. If the ratio d_0 / d_1 is within a certain threshold range (0.8 in this paper), it is considered to be successful to match the two feature points which can calculate the nearest neighboring Euclidean distance. Otherwise, the first image will be traversed to search for the common point of the next feature point, until the common points in the first image are traversed completely, obtaining N pairs of matching common points.

Secondly, the linear slope constraint is used to filter the matching point-pairs having large difference in slope values. By calculating the vector direction of the line connecting the common points extracted by the ratio purification method, we can confirm the slope k_m of any line connecting a pair of the common points. In the process of calculating the slope values, after converting the angles with negative slope to positive angles by adding $180°$, every $3°$ is used as a quantitative index to accumulate the angle values of all common points into 60 classifications. In the statistical classifications, the slope angle value of the common points with the most number is searched, and its corresponding slope value is selected as rejection threshold, k_m, to delete the feature point-pairs whose angle of slope is different from the angle of k_m more than $3°$.

Finally, the RANSAC algorithm is adopted to further eliminate outer points of the common points, and the corresponding transformation matrix model is obtained. The process is as follows:

The RANSAC algorithm is utilized to determine the initial transformation matrix. The coordinates of the corresponding common points on two adjacent images are marked as I_i and

I_{i+1} respectively, $I_i = (x_i, y_i, 1)^T$, $I_{i+1} = (x_{i+1}, y_{i+1}, 1)^T$. The corresponding relationship between the common points on two images can be expressed as follows:

$$I_i = HI_{i+1} \tag{1}$$

$$\mathrm{H} = \begin{bmatrix} h_0 & h_1 & h_2 \\ h_3 & h_4 & h_5 \\ h_6 & h_7 & 1 \end{bmatrix} \tag{2}$$

H is the expression of the transformation matrix; h_0, h_1, h_3, h_4 are the image scaling and rotation values; h_2, h_5 are the horizontal and vertical displacement quantities respectively; h_6, h_7 are the horizontal and vertical deformation quantities respectively.

The transformation matrix H needs to solve eight parameters, so four common point-pairs would be enough. The RANSAC algorithm adopts iteration method to solve the initial transformation matrix, and before solving the matrix, three parameters (error threshold, iteration times and inner points' number threshold) determining the inner points should be installed ahead. In every iteration, four common points are randomly selected to calculate a transformation matrix H. Equation 1 is used to transform the feature points of the second image to the coordinate of the first image, and the variation errors between common points are calculated after transformation. If variation errors are within the configured error threshold of inner points, it is considered that this pair of common points is an inner point-pair. Then the number of inner points is counted, and if this number is within the configured number threshold of inner points, the solved H will be obtained as the initial transformation matrix; otherwise, the iteration continues.

Then, we utilize the nonlinear least square L-M algorithm [20] to solve the transformation matrix with high accuracy based on the initial transformation matrix, so as to reduce the influence of the accumulative errors and noise, and improve the mosaic quality. The least square L-M algorithm is adopted to solve the optimal parameters of the transformation matrix H, so that the function $F(h)$ using parameters of the transformation matrix as variables can acquire the minimum value. The function $F(h)$ represents the sum of distances between all matching common points, as Equation 3 and Equation 4:

$$\mathrm{F}(\mathrm{h}) = \sum_j \left[\left(\frac{h_0 x_i + h_1 y_i + h_2}{h_6 x_i + h_7 y_i + 1} - x_i^{'} \right)^2 + \left(\frac{h_3 x_i + h_4 y_i + h_5}{h_6 x_i + h_7 y_i + 1} - y_i^{'} \right)^2 \right]^{\frac{1}{2}} \tag{3}$$

x_i, y_i represent the coordinates of the feature points in one of the two adjacent images, and x_i', y_i', matched to x_i, y_i, represent the coordinates of the feature points in the other image.

$$\mathrm{f}_j(\mathrm{h}) = \left[\left(\frac{h_0 x_i + h_1 y_i + h_2}{h_6 x_i + h_7 y_i + 1} - x_i' \right)^2 + \left(\frac{h_3 x_i + h_4 y_i + h_5}{h_6 x_i + h_7 y_i + 1} - y_i' \right)^2 \right]^{\frac{1}{2}} \tag{4}$$

$\mathrm{f}_j(\mathrm{h})$ represents the component in the latter part of Equation 3, namely, $\mathrm{F}(\mathrm{h}) = \sum_j f_j(h)$.

Under the condition of a given accuracy parameter ε, the iteration method is used to minimize the transformation matrix H, and the process is shown as the Equation 5:

$$h_{k+1} = h_k + h_{LM} \tag{5}$$

h_k, h_{k+1} represent the transformation matrices, ranges from 0; h_0 represents the initial transformation matrix; h_{LM} is an expression shown as Equation 6:

$$h_{LM} = -\left(J(h)^T J(h) + \mu I \right)^{-1} J(h)^T f(h) \tag{6}$$

μ is a constant greater than zero, generally set $\mu = 0.01$; h is a variable set, representing the parameters , $h_0, h_1, \cdots$, of the transformation matrix; $J(h)$ represents the partial differential Jacobian matrix of function f on the matrix parameters $h_0, h_1, \cdots$, as Equation 7:

$$J(h) = \begin{vmatrix} \frac{\partial f_1}{\partial h_0} & \frac{\partial f_1}{\partial h_2} & \cdots & \frac{\partial f_1}{\partial h_7} \\ \frac{\partial f_2}{\partial h_0} & \frac{\partial f_2}{\partial h_1} & \cdots & \frac{\partial f_2}{\partial h_7} \\ \vdots & \vdots & \vdots & \vdots \\ \frac{\partial f_n}{\partial h_0} & \frac{\partial f_n}{\partial h_1} & \cdots & \frac{\partial f_n}{\partial h_7} \end{vmatrix} \tag{7}$$

$\frac{\partial \mathrm{f}_n}{\partial \mathrm{h}_0}, \frac{\partial f_n}{\partial h_1}, \cdots \frac{\partial f}{\partial h_7}$ represent that multi-variable function $f_n(h)$ takes the partial differential on every argument from h_0 to h_7, n ranging from 0 to K, and K representing the iteration times.

After K times ($K \geq 3$) iteration calculation, we can obtain the transformation matrix, $H = h_{k+1}$, with relatively high accuracy. Using this matrix can reduce the effect of accumulative errors and noise in the process of image mosaic, and improve the precision of image mosaic.

2.4 Image Mosaic and Fusion

Using the transformation matrix H, each single frame image is transformed respectively into the same coordinate system. Then the images are reassigned to synthesize on the result image by the nearest neighbor interpolation or the bilinear interpolation. The mosaic of images is basically completed, and we can obtain a result image with wide view field.

In order to avoid the "ghosting" phenomenon appearing on the overlapping area of adjacent images, conventional methods directly cover the previous image with the other one. However, influenced by several factors (imaging time, different conditions of atmospheric radiation and light, etc.) of each image, it has color aberration in vision in the images. Consequently, the conventional covering methods would lead to obvious gray scale differences in the overlapping areas between adjacent images.

Image fusion is designed to solve the above problem to make a smooth transition between adjacent mosaic images and achieve a good visual effect. According to the basic commonsense that the pixel distortion at the central point of the plane array camera is the smallest, we calculate dis_0 and dis_1, the distances between the pixel $I(x,y)$ in overlapping area and the central points of two adjacent images, respectively. dis_0 and dis_1 are utilized to obtain ρ_i – the weight of pixels in the fusion image, so as to confirm the pixel value $f(x,y)$ of the overlapping area after fusion. The expression of ρ_i is as follows:

$$\rho_i = \frac{1}{1+\left(\frac{dis_0}{dis_1}\right)^{\lambda}} \tag{8}$$

$I(x,y)$ represents the pixel value of the overlapping area $I(x,y)$ in the first image, $WI_1(x,y)$ represents the Gauss weighted value of $I_1(x,y)$ within a 3×3 neighborhood in the first image; $I_2(x,y)$ represents the pixel value of overlapping area in the second image, $WI_2(x,y)$ represents the Gauss weighted value of $I_2(x,y)$ within a 3×3 neighborhood in the second image. The expressions are as follows:

$$WI_1(x,y) = \sum_{i=1}^{9}\left(I_1(x_i,y_i) * \frac{1}{2\pi\sigma^2} e^{-\frac{x_i^2+y_i^2}{2\sigma^2}} \right) \tag{9}$$

$$WI_2(x,y)=\sum_{i=1}^{9}\left(I_2(x_i,y_i)*\frac{1}{2\pi\sigma^2}e^{-\frac{x_i^2+y_i^2}{2\sigma^2}}\right) \tag{10}$$

The pixel value of the overlapping area after fusion is as follows:

$$f(x,y)=\begin{cases}WI_1(x,y)\times\rho_i+WI_2(x,y)\times(1-\rho_i) & dis_0>dis_1\text{且}I_1(x,y)\neq 0,\ I_2(x,y)\neq 0\\ WI_1(x,y)\times(1-\rho_i)+WI_2(x,y)\times\rho_i & dis_0<dis_1\text{且}I_1(x,y)\neq 0,\ I_2(x,y)\neq 0\\ I_1(x,y) & I_1(x,y)\neq 0,\ I_2(x,y)=0\\ I_2(x,y) & I_1(x,y)=0,\ I_2(x,y)\neq 0\end{cases} \tag{11}$$

III. RESULTS AND DISCUSSION

3.1 Data Set

In our experiments, a medium-altitude UAV is employed. The main types of landforms include city, village, open field, etc. Infrared camera, visible-light camera and digital camera are mounted on the UAV, generating three types of data, infrared video, visible-light video and digital photograph. The resolution of each type of data is shown in Table 2.

Table 2. Resolution of each type of data

Data type	Resolution
Infrared video	720×576
Visible-light video	1392×1040
Digital photograph	5616×3744

3.2 Experiment for Three-step Registration

In this experiment, we use some images from infrared video to verify the proposed three-step registration method. The detection effects of SIFT feature points in two images are shown in Fig. 3a and Fig. 3b.

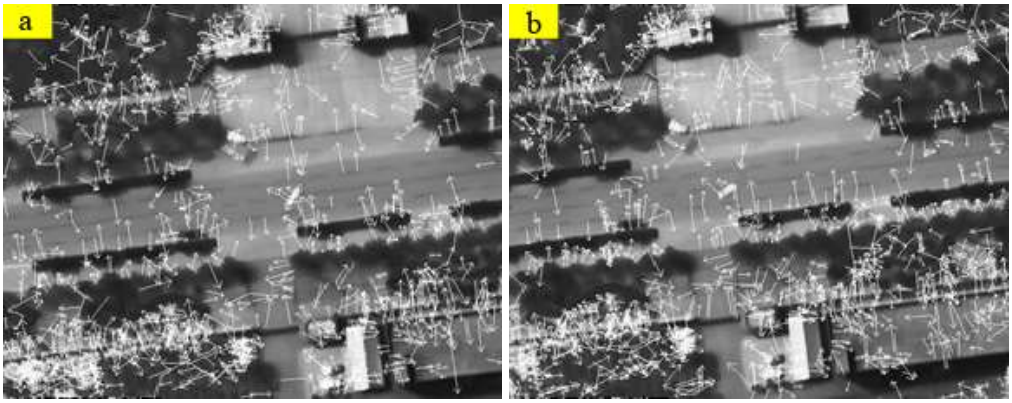

Figure 3. The SIFT feature points detection.
(a) SIFT feature points of Image 1 (b) SIFT feature points of Image 2

The Euclidean distance is calculated by the descriptor (128 dimension vector) of two adjacent images' feature points, to achieve the coarse matching of feature points. The matching results are shown in Figure 4a and Figure 4b: the Figure 4a shows the coarse matching results of Figure 3a and Figure 3b; the Figure 4b shows the error matching results in Figure 3a and Figure 3b. A slope constraint method is used to remove the matching point-pairs with large difference in slope values, and the matching results are shown in Figure 4c, where the error matching points are basically eliminated.

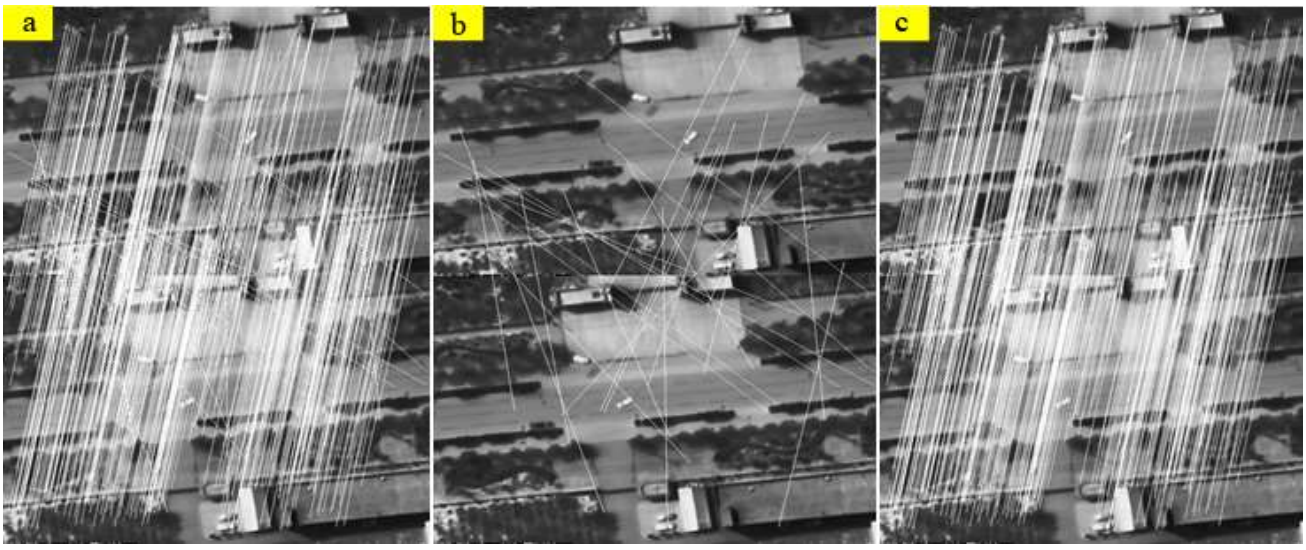

Figure 4. The matching results. (a) The coarse matching results (b) The error matching results
(c) The matching results after slope constraint

The RANSAC algorithm is adopted to further eliminate the outer points of the common points and obtain the corresponding transformation model matrix. After being dealt with ratio purification and slope constraint, most mismatching feature point-pairs are eliminated, reducing the computation of RANSAC algorithm. Meanwhile, in the process of every random sampling, the RANSAC algorithm can obtain the model transformation matrix H with relatively high accuracy and remove the outer points effectively, so that the matching accuracy is further improved, which lays a good foundation for the final fusion of the result image. As shown in Figure 5a, the mosaic image without being dealt with the slope constraint method has several obvious mosaic seam dislocations. Figure 5b shows that after being dealt with the three-step registration method, the mosaic dislocation phenomenon disappears.

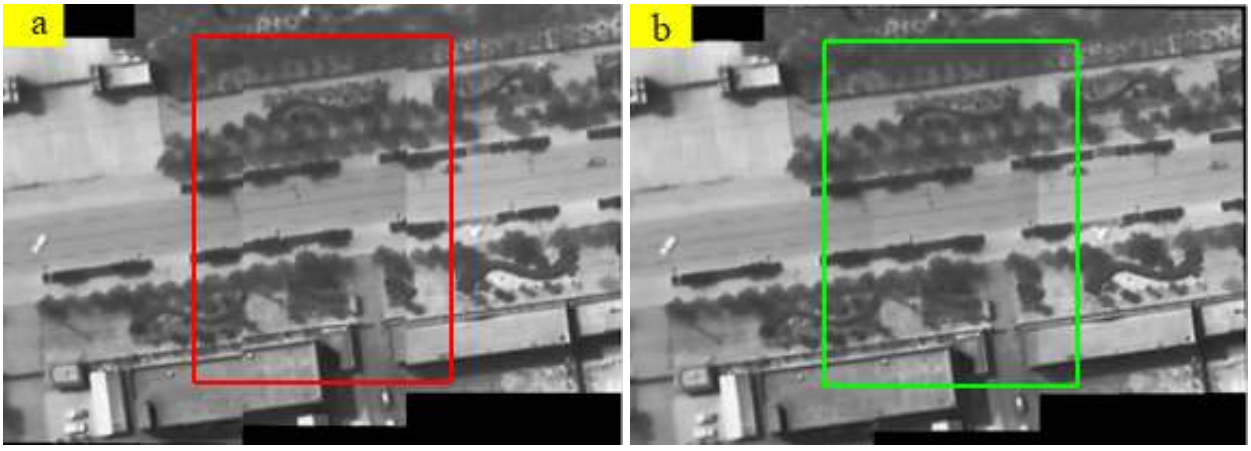

Figure 5. The mosaic results. (a)Image without being dealt with slope constraint (b) Image dealt with the three-step registration method

The images taken from UAV infrared video is mosaicked by the three-step registration algorithm, and the panoramic image is shown as Figure 6. There is no visible dislocation in mosaicking seams, suggesting that the mosaicking precision is pretty encouraging. This experiment proves the validity of the three-step registration method proposed in this paper.

Figure 6. The mosaic result of infrared images

3.3 Experiment for Multi-Thread Processing

In the whole process of image mosaic, feature extraction speed has a decisive impact on the real-time capability of the algorithm. We adopt the multi-thread processing in Section 2.3. In order to test the performance of multi-thread processing algorithm, we use the computer, with 2G internal memory and 2 cores of E4600 processor, to implement mosaic experiments on three groups of images from different types of data. The analysis of performance in multi-thread processing is shown in Table 3, and the time consumption of multi-thread method is greatly reduced in three groups of experiments. The speed with best performance increases by 75.4%, and the average speed increases by 69.8%, presenting the superiority of multi-thread method.

Table 3. Resolution of each type of data

Group ID	Data type	Number of images	Time consumption of Single-Thread (t1=seconds / frame)	Time consumption of Multi-Thread (t2=seconds / frame)	Improvement Percentage (1-t2/t1)
1	Infrared video	1000	1.247	0.305	75.4%
2	Visible-light video	1000	6.52	2.14	67.2%
3	Digital photograph	300	27.4	9.08	66.8%

The algorithm proposed in this paper combines the three-step registration method with multi-thread processing, and the analysis of the whole image mosaic algorithm is as follows. Three

types of image sets, namely, 1000 images derived from infrared video, 1000 images derived from visible-light video and 300 images derived from digital photograph, are mosaicked by the proposed algorithm, and several sections of the mosaic results are shown as Figure 7, Figure 8 and Figure 9, respectively. There is no visible dislocation in mosaicking seams, suggesting that the mosaicking precision is quite encouraging.

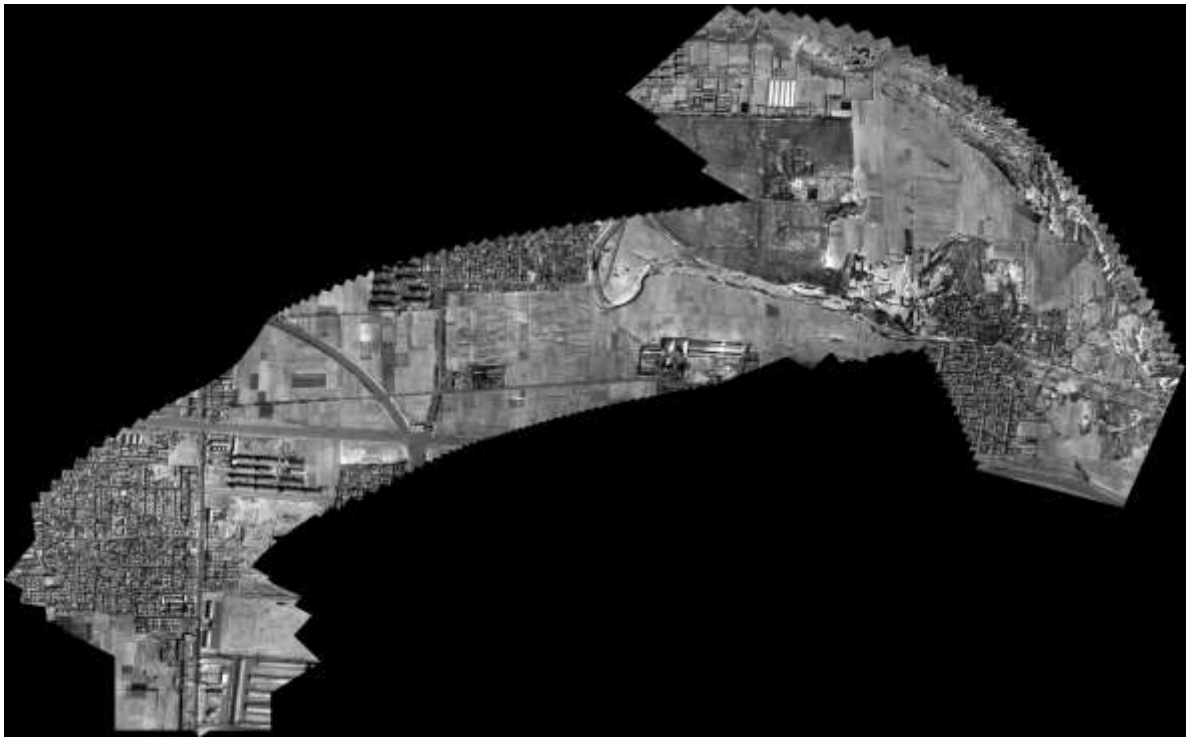

Figure 7. The mosaic result of infrared images

Figure 8. The mosaic result of visible-light images

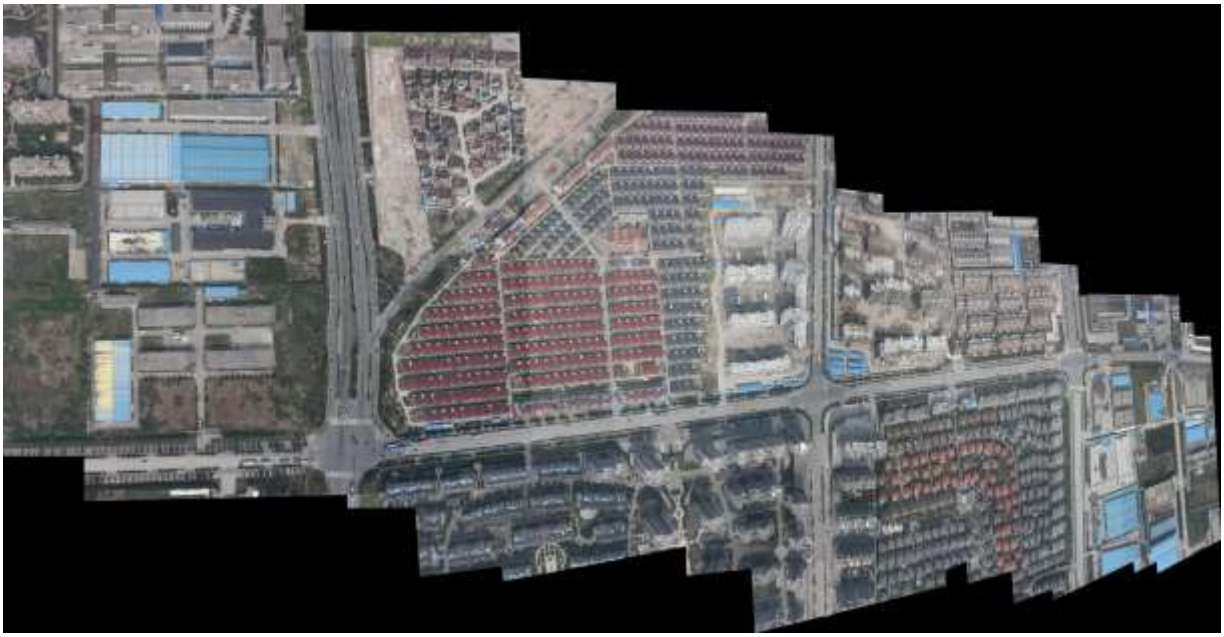

Figure 9. The mosaic result of digital photographs

To verify the performance in speed, a comparison about the average time consumption of per frames (seconds/frame) between the proposed algorithm with the conventional algorithm based on SIFT [5] was implemented, and the results of different types of image data are as shown in Figure 10, Figure 11 and Figure 12, respectively.

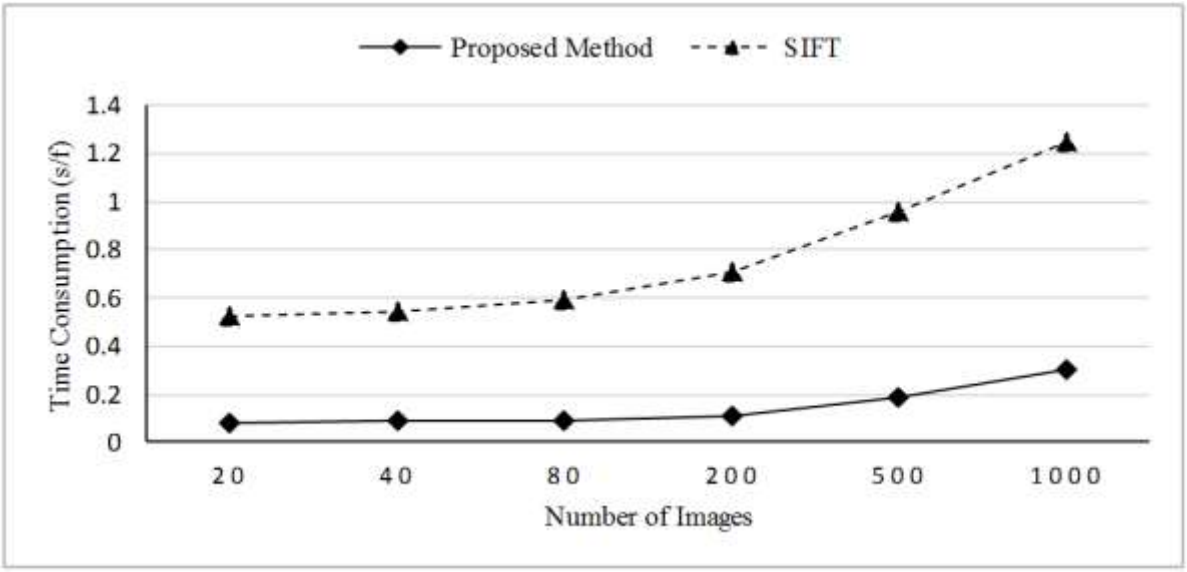

Figure 10. The average time consumption of infrared images

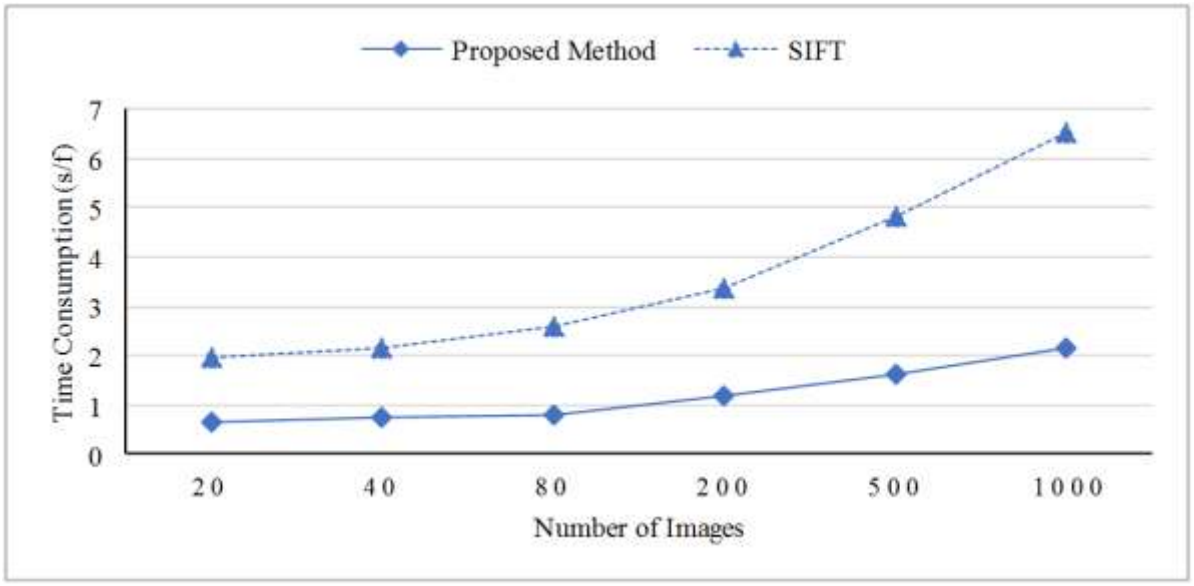

Figure 11. The average time consumption of visible light images

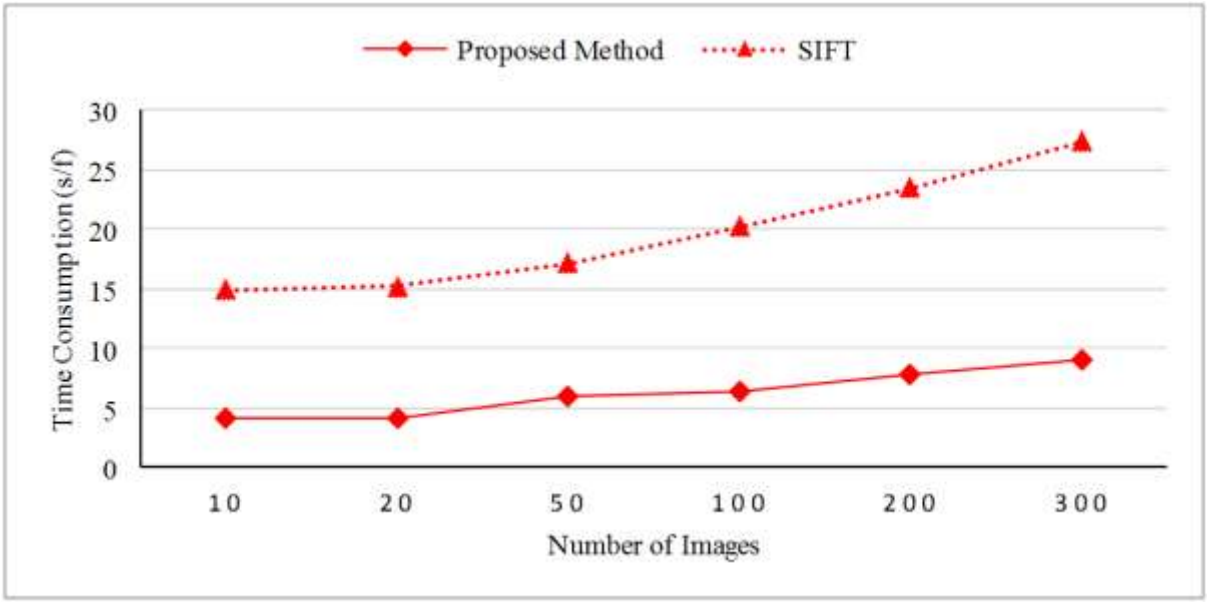

Figure 12. The average time consumption of digital photographs

With the number of images increasing, the amount of calculation increases gradually, and the average time consumption of per image correspondingly rises. And the larger number of images is, the gap of average time consumption between the proposed algorithm and the basic SIFT algorithm is more obvious, showing the efficiency of the proposed algorithm in speed increasing. Consequently, the experimental results show that the method proposed in this paper is quite encouraging in the performance of speed and precision.

IV. CONCLUSIONS

Image mosaic is a significant technology to convert massive images with small field of view into images with wide field of view. There are two vital problems of image mosaic, the mosaic seam dislocations caused by registration error, and the poor real-time capability caused by large calculation.

In order to solve the mosaic precision problem of mosaic seam dislocations caused by error accumulation, a novel three-step registration algorithm is proposed in this paper. The algorithm is based on the SIFT features, and has some contributions on more accurate registration. Aiming at the problem of poor real-time capability caused by large amount of calculation, this paper designs a new pattern of data processing to utilize the multi-core resources and multi-thread computing method of computers, which is in accordance with the characteristics and requirements of UAV's image mosaic processing with large calculation. Using some image data acquired by a medium altitude UAV, this paper designs the precision verification experiments and the time consumption verification experiments. The experimental results suggest that the method proposed in this paper can effectively eliminate mosaicking errors and greatly improve the mosaicking speed of the whole algorithm. Consequently, it could enhance the mosaic processing ability to deal with the UAV surveillance images with large calculation, ensuring the real-time generation of mosaic image products for UAV applications.

AKNOWLEDGEMENT

This work has been supported by the National Natural Science Foundation of China (NO. 61450008) and Aerospace Science and Technology Innovation Fund and Aerospace Science & Technology Innovation Fund.

REFERENCES

[1] Niethammer U, James M R, Rothmund S, et al., "UAV-based remote sensing of the Super-Sauze landslide: Evaluation and results", Engineering Geology, 2012, 128(11):2-11.

[2] Yanmin L, Peizhong L, et al., "An artificial immune network clustering algorithm for mangroves remote sensing image", International Journal on Smart Sensing & Intelligent Systems, 2014, 7(1): 116 – 134.

[3] Feng Q, Liu J, Gong J., "Urban Flood Mapping Based on Unmanned Aerial Vehicle Remote Sensing and Random Forest Classifier—A Case of Yuyao, China", Water, 2015, 7(4):1437-1455.

[4] Watts A C, Ambrosia V G, Hinkley E A., "Unmanned Aircraft Systems in Remote Sensing and Scientific Research: Classification and Considerations of Use", Remote Sensing, 2012, 4(6):1671-1692.

[5] Lowe D G. Distinctive Image Features from Scale-Invariant Keypoints// International Journal of Computer Vision. 2004:91-110.

[6] Brown M, Lowe D G. Automatic panoramic image stitching using invariant features// International Journal of Computer Vision. 2007:59-73.

[7] Abdel-Hakim A E, Farag A. CSIFT: A SIFT Descriptor with Color Invariant Characteristics// IEEE Computer Society Conference on Computer Vision & Pattern Recognition (CVPR), 2006:1978-1983.

[8] Zeng L, Zhang S, Zhang J, et al., "Dynamic image mosaic via SIFT and dynamic programming", Machine Vision & Applications, 2014, 25(5):1271-1282.

[9] Bay H, Ess A, Tuytelaars T, et al., "Speeded-Up Robust Features (SURF)[J]. Computer Vision & Image Understanding,", 2008, 110(3):346-359.

[10] Rublee E, Rabaud V, Konolige K, et al., "ORB: An efficient alternative to SIFT or SURF", Proceedings, 2011, 58(11):2564-2571.

[11] Yang Y, Sun G, Zhao D, et al., "A Real Time Mosaic Method for Remote Sensing Video Images from UAV ", Journal of Signal & Information Processing, 2013, 04(3B):168-172.

[12] Haripriya Y, Bindu Pavani K V, Lavanya S, et al., "Feature Based Image Stitching on Aerial Images", International Journal of Applied Engineering Research, 2013.

[13] Wang H, Li J, Wang L, et al., "Automated mosaicking of UAV images based on SFM method", Geoscience and Remote Sensing Symposium (IGARSS), 2014 IEEE International. IEEE, 2014:2633 - 2636.

[14] Zhouping Y., "Fusion algorithm of optical images and SAR with SVT and sparse representation", International Journal on Smart Sensing & Intelligent Systems, 2015, 8(2):1123-1141.

[15] Jansson J, Gustafsson F., "Image Stitching Using Structure Deformation", IEEE Transactions on Pattern Analysis & Machine Intelligence, 2008, 30(4):617-631.

[16] Chandratre R, A Chakkarwar V., “Image Stitching using Harris and RANSAC”, International Journal of Computer Applications, 2014, 89(15):14-19.

[17] Yongjin Y, Xinmei Z, et al., “Research of Image Pre-processing Algorithm Based on FPGA”, International Journal on Smart Sensing & Intelligent Systems, 2013, 6(4): 1499 – 1515.

[18] Nistér D. Preemptive RANSAC for live structure and motion estimation, Computer Vision, 2003. Proceedings, Ninth IEEE International Conference on. IEEE, 2003:199-206 vol.1.

[19] Beis J S, Lowe D G., “Shape Indexing Using Approximate Nearest-Neighbour Search in High-Dimensional Spaces”, Proceedings of the 1997 Conference on Computer Vision and Pattern Recognition (CVPR '97). IEEE Computer Society, 1997:1000.

[20] Lourakis M I A., “A Brief Description of the Levenberg-Marquardt Algorithm Implemened by levmar”, Foundation of Research & Technology, 2005.